

CH₂CO)⁺. Anal. Calcd for C₁₆H₁₆N₂O₃: C, 67.59; H, 5.67; N, 9.85. Found: C, 67.43; H, 6.11; N, 9.91.

5 (Ar₁ = Ph, Ar₂ = *p*-CH₃OC₆H₄): IR (ν_{CO}) 1695, 1678 cm⁻¹; ¹H NMR (CDCl₃) δ 1.90 (s, 6 H, COCH₃), 3.73 (s, 3 H, OCH₃), 6.56–7.27 (m, 9 H, aromatic protons); MS (*m/e*) 298 [M]⁺, 256 [M – COCH₂]⁺. Anal. Calcd for C₁₇H₁₈N₂O₃: C, 68.44; H, 6.08, N, 9.39. Found: C, 68.50; H, 5.77, N, 9.23.

5 (Ar₁ = Ar₂ = *p*-CH₃OC₆H₄): IR (ν_{CO}) 1694, 1673 cm⁻¹; ¹H NMR (CDCl₃) δ 1.88 (s, 6 H, COCH₃), 3.70 (s, 6 H, OCH₃), 6.63–6.90 (m, 8 H, aromatic protons); MS (*m/e*) 164 [M]⁺, 122 [M – COCH₂]⁺; mp 120–122 °C. Anal. Calcd for C₁₈H₂₀N₂O₄: C, 65.84; H, 6.14; N, 8.53. Found: C, 65.74; H, 6.01; N, 8.83.

General Procedure for the Acylation of Azoarenes by Co₂(CO)₈ and *p*-TsOH. A mixture of distilled water (24 mL), benzene (24 mL), and *p*-TsOH (see Table II for amount) was degassed at 60 °C with use of nitrogen. The gas was changed to carbon monoxide and Co₂(CO)₈ (0.68 g, 2.0 mmol) and methyl iodide (3.0 mL, 62 mmol) were added, followed 30 min later by 2.0 mmol of the azo compound. The reaction mixture was stirred overnight at 60 °C under carbon monoxide. The cooled mixture was filtered, the layers were separated, and the aqueous phase was neutralized and extracted with an equal volume of chloroform. The combined organic phase was dried (MgSO₄) and concentrated. Purification of the resulting crude product was effected by silica gel chromatography with 7/3 or 1/1 hexane/ethyl acetate as the eluant.

Data for 8 (Ar₁ = Ar₂ = Ph): IR (ν_{CO}) 1673 cm⁻¹; ¹H NMR (CDCl₃) δ 2.22 (s, 3 H, CH₃), 6.55–7.69 (m, 11 H, aromatic protons and NH); MS (*m/e*) 226 [M]⁺, 183 [M – COCH₃]⁺; mp 132–133 °C. Anal. Calcd for C₁₄H₁₄N₂O: C, 74.31; H, 6.24; N, 12.38. Found: C, 74.27; H, 6.30; N, 12.72.

8 (Ar₁ = Ar₂ = *p*-CH₃C₆H₄): IR (ν_{CO}) 1672 cm⁻¹; ¹H NMR (CDCl₃) δ 2.23 (s, 3 H, COCH₃), 2.26 (s, 6 H, *p*-CH₃C₆H₄), 6.53–7.26 (m, 9 H, aromatic and amino protons); MS (*m/e*) 254 [M]⁺, 211 [M – COCH₃]⁺; mp 141–142 °C. Anal. Calcd for C₁₆H₁₈N₂O: C, 75.56; H, 7.13; N, 11.01. Found: C, 75.21; H, 7.33; N, 10.63.

8 (Ar₁ = Ar₂ = *m*-CH₃C₆H₄): IR (ν_{CO}) 1672 cm⁻¹; ¹H NMR (CDCl₃) δ 2.22 (s, 3 H, COCH₃), 2.26 (s, 6 H, *m*-CH₃C₆H₄),

6.56–7.30 (m, 9 H, aromatic and amino protons); MS (*m/e*) 254 [M]⁺, 211 [M – COCH₃]⁺; mp 129–130 °C. Anal. Calcd for C₁₆H₁₈N₂O: C, 75.56; H, 7.13; N, 11.01. Found: C, 75.93; H, 7.12; N, 11.09.

8 (Ar₁ = Ar₂ = *p*-ClC₆H₄): IR (ν_{CO}) 1678 cm⁻¹; ¹H NMR (CDCl₃) 2.16 (s, 3 H, COCH₃), 6.50–7.33 (m, 9 H, aromatic and amino protons); MS (*m/e*) 298, 296, 294 [M]⁺; mp 94–96 °C.

8 (Ar₁ = Ar₂ = C₅H₁₀NCO): IR (ν_{CO}) 1680 cm⁻¹; ¹H NMR (CDCl₃) δ 1.36–1.83 (m, 12 H, C(CH₂)₃C), 2.09 (s, 3 H, COCH₃), 3.38 (m, 8 H, CH₂NCH₂), 8.33 (s, 1 H, NH); MS (*m/e*) 296 [M]⁺; mp 153–154 °C. Anal. Calcd for C₁₄H₂₄N₄O₃: C, 56.71; H, 8.17; N, 18.91. Found: C, 56.93; H, 8.10; N, 18.65.

Acknowledgment. We are grateful to the Natural Sciences and Engineering Research Council for Support of this research. D.R. is indebted to the NSERC for a predoctoral fellowship.

Registry No. 4 (Ar₁ = Ar₂ = Ph), 103-33-3; 4 (Ar₁ = Ar₂ = *p*-MeC₆H₄), 501-60-0; 4 (Ar₁ = Ar₂ = *m*-MeC₆H₄), 588-04-5; 4 (Ar₁ = Ar₂ = *p*-ClC₆H₄), 1602-00-2; 4 (Ar₁ = Ph, Ar₂ = *p*-MeOC(O)C₆H₄), 2918-88-9; 4 (Ar₁ = Ph, Ar₂ = *p*-HOC₆H₄), 1689-82-3; 4 (Ar₁ = Ph, Ar₂ = *p*-MeOC₆H₄), 2396-60-3; 4 (Ar₁ = Ar₂ = *p*-MeOC₆H₄), 501-58-6; 4 (Ar₁ = Ar₂ = C₅H₁₀NC(O)), 10465-81-3; 4 (Ar₁ = Ph, Ar₂ = *p*-AcOC₆H₄), 13102-31-3; 5 (Ar₁ = Ar₂ = Ph), 6049-42-9; 5 (Ar₁ = Ar₂ = *p*-MeC₆H₄), 125879-54-1; 5 (Ar₁ = Ar₂ = *m*-MeC₆H₄), 125879-55-2; 5 (Ar₁ = Ar₂ = *p*-ClC₆H₄), 125879-56-3; 5 (Ar₁ = Ph, Ar₂ = *p*-MeOC(O)C₆H₄), 125879-57-4; 5 (Ar₁ = Ph, Ar₂ = *p*-AcOC₆H₄), 125879-58-5; 5 (Ar₁ = Ph, Ar₂ = *p*-HOC₆H₄), 125879-59-6; 5 (Ar₁ = Ph, Ar₂ = *p*-MeOC₆H₄), 125879-60-9; 5 (Ar₁ = Ar₂ = *p*-MeOC₆H₄), 125879-61-0; 6 (Ar₁ = Ph), 103-84-4; 7 (Ar₂ = *p*-HOC₆H₄), 103-90-2; 7 (Ar₂ = *p*-MeOC₆H₄), 51-66-1; 8 (Ar₁ = Ar₂ = C₅H₁₀NC(O)), 125879-62-1; 8 (Ar₁ = Ar₂ = Ph), 22293-38-5; 8 (Ar₁ = Ar₂ = *p*-MeC₆H₄), 125879-63-2; 8 (Ar₁ = Ar₂ = *m*-MeC₆H₄), 125879-64-3; 8 (Ar₁ = Ar₂ = *p*-ClC₆H₄), 125879-65-4; 8 (Ar₁ = Ar₂ = C₅H₁₀NC(O)), 125879-62-1; Co₂(CO)₈, 10210-68-1; Me-*m*-C₆H₄NHNHC₆H₄-*m*-Me, 621-26-1; Cl-*p*-C₆H₄NHNHC₆H₄-*p*-Cl, 953-14-0.

Thermochemistry of C–H and C–C Bond Activation: Translational Energy Dependence of Reactions of Sc⁺ with Propane and 2-Butenes

L. S. Sunderlin and P. B. Armentrout*[†]

Department of Chemistry, University of Utah, Salt Lake City, Utah 84112

Received September 13, 1989

Selected reactions of Sc⁺ with propane and *cis*- and *trans*-2-butene are studied by using a guided ion beam mass spectrometer. The results show reaction efficiencies at low energies of ≈100% with butene but only ≈5% with propane. The thresholds for formation of ScCH₄⁺ and ScC₂H₆⁺ are used to determine the two-ligand bond dissociation energies $D^{\circ}(\text{Sc}^+-\text{H}) + D^{\circ}(\text{HSc}^+-\text{CH}_3) = 120 \pm 2$ kcal/mol and $D^{\circ}(\text{Sc}^+-\text{CH}_3) + D^{\circ}(\text{CH}_3\text{Sc}^+-\text{CH}_3) = 117 \pm 2$ kcal/mol. These values are comparable to $D^{\circ}(\text{Sc}^+-\text{H}) + D^{\circ}(\text{HSc}^+-\text{H}) = 116 \pm 3$ kcal/mol determined previously and are consistent with bond additivity arguments based on orbital occupations in these molecules. Implications for the thermochemistry of covalent bond activation processes are discussed.

Introduction

One of the important contributions that studies of gas-phase transition metal chemistry can make to organometallic chemistry is the measurement of bond dis-

sociation energies. At present, bond strengths between first-row transition-metal ions and one ligand (e.g., M⁺-H, M⁺-CH₂, and M⁺-CH₃) are reasonably well established,¹ but far fewer bond energies are known for attachment in

[†] NSF Presidential Young Investigator 1984–1989; Alfred P. Sloan Fellow; Camille and Henry Dreyfus Teacher-Scholar, 1988–1993.

(1) Armentrout, P. B.; Georgiadis, R. *Polyhedron* 1988, 7, 1573–1581. Armentrout, P. B.; Sunderlin, L. S.; Fisher, E. R. *Inorg. Chem.* 1989, 28, 4436–4437.

the reactions of metal ions with neutrals in the gas phase. Understanding the thermochemistry of such two-ligand species is an important step in linking gas-phase metal-ligand thermochemistry to "real world" condensed-phase systems. In particular, such two-ligand bond energies are directly related to the energetics of the fundamental reaction of insertion into bonds (oxidative addition).

One metal that readily produces two-ligand species is Sc^+ . Previous work has elucidated the reactions of Sc^+ with H_2 ,^{2,3} CH_4 ,⁴ C_2H_6 ,³⁻⁵ larger hydrocarbons,³ and alkenes.⁶ These reports indicate that Sc^+ shows "unique reactivity" among the first-row transition metals, reactivity that includes the formation of two-ligand products. As yet, however, only the dihydride of scandium has been quantitatively characterized.^{4,5} In this paper, we examine several reaction systems to similarly characterize HScCH_3^+ and $\text{Sc}(\text{CH}_3)_2^+$. Our intent is to better understand the thermochemistry of oxidative addition of hydrocarbons to transition-metal centers. Similar work on the reactions of Ti^+ with these neutrals and the thermochemical properties of $\text{Ti}(\text{CH}_3)_2^+$ has also recently been published.⁷

Experimental Section

A complete description of the apparatus and experimental procedures is given elsewhere.⁸ In the ion source, $\text{ScCl}_3 \cdot 6\text{H}_2\text{O}$ (Aesar) is vaporized in an oven and directed toward a resistively heated rhenium filament where the metal halide decomposes and the resulting metal atoms are ionized by surface ionization (SI). It is generally assumed that a Maxwell-Boltzmann distribution accurately describes the populations of the electronic states of ions produced by SI. The validity of this has been discussed in detail.⁹ At the typical filament temperature of 2250 K, 88% of the Sc^+ ions are in the $a^3\text{D}(4s3d)$ ground state, 6% are in the $a^1\text{D}(4s3d)$ state at 0.32 eV, and 6% are in the $a^3\text{F}(3d^2)$ state at 0.61 eV. Less than 0.1% are in higher excited states at 1.36 eV and above.¹⁰

The resulting ions are focused into a magnetic sector momentum analyzer for mass analysis. The mass-selected Sc^+ ions are then decelerated to a desired kinetic energy and focused into an octopole ion guide that traps ions over the mass range studied. The octopole passes through a static gas cell into which reactant gasses are introduced. Pressures are maintained at a sufficiently low level (<0.1 mTorr) that multiple ion-molecule collisions are improbable. Product and unreacted beam ions are contained in the guide until they leave the gas cell. The ions are then focused into a quadrupole mass filter for product mass analysis and detected. Raw ion intensities are converted to absolute cross sections as described previously.⁸ The accuracy of our absolute cross sections is estimated to be $\pm 20\%$.

The absolute energy and the energy distribution of the ions are measured by using the octopole as a retarding field analyzer. The fwhm of the energy distribution is generally 0.6 eV in the laboratory frame for these reactions. Uncertainties in the absolute energy scale are ± 0.05 eV lab. Translational energies in the laboratory frame of reference are related to energies in the center of mass (CM) frame by $E_{\text{CM}} = E_{\text{lab}}m/(M+m)$, where M and m are the masses of the incident ion and neutral reactant, respec-

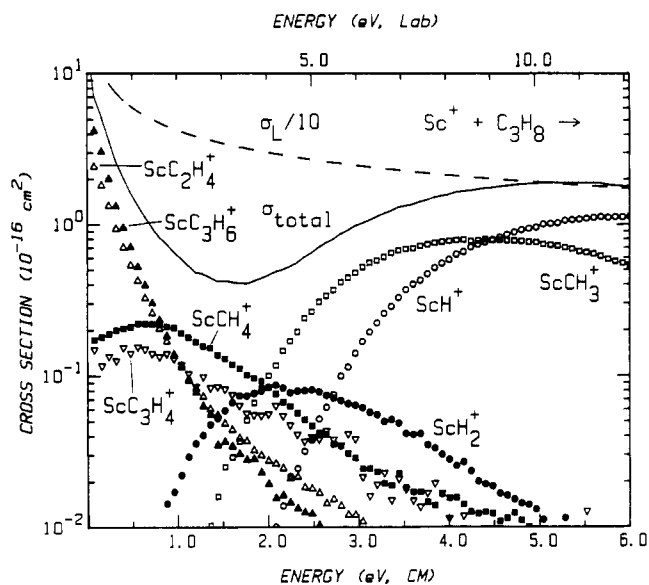
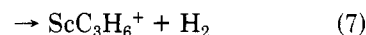
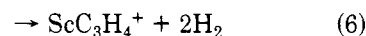
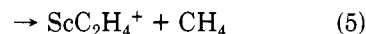
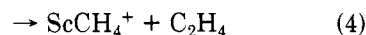
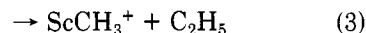
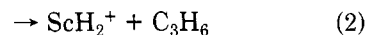
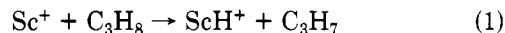


Figure 1. Variations of product cross sections with translational energy in the laboratory frame (upper axis) and center-of-mass frame (lower axis) for the reaction of Sc^+ with propane.

tively. The data obtained in this experiment are broadened by the ion energy spread mentioned above and Doppler broadening, which has a width (in electronvolts) in the CM frame of $\approx 0.37E^{1/2}$ for both reaction systems.¹¹ When model cross sections are compared to experimental data, the calculated cross sections are convoluted with both sources of experimental energy broadening.

Results

Propane. The major products seen in the reaction of Sc^+ with propane are given in reactions 1–7. Cross sec-



tions for these reactions are shown in Figure 1. Other products seen are ScCH_2^+ , ScC_2H_2^+ , ScC_2H_3^+ , and ScC_2H_5^+ . These reactions have cross sections $\leq 0.1 \text{ \AA}^2$ over the energy range studied.

Also plotted in Figure 1 is the total reaction cross section and the Langevin cross section for close collisions between the reactants, σ_L . This latter cross section is given by $\sigma_L = \pi e(2\alpha/E)^{1/2}$, where e is the charge of the ion, α is the polarizability of the neutral, and E is the translational energy. This comparison shows that the overall reaction efficiency is around 5% at low energy.

The main reactions at low energies are single and double dehydrogenation and demethanation, reactions 7, 6, and 5, respectively. Tolbert and Beauchamp (TB) in an earlier study of this system found a branching ratio for formation of ScC_2H_4^+ , ScC_3H_4^+ , and ScC_3H_6^+ of 27:5:68 at 0.5 eV, with a total cross section of $\approx 7 \text{ \AA}^2$ at that energy.³ These results are most consistent with our data at 0.25 eV, where we measure a ratio of 36:4:55:5 for these three products and ScCH_4^+ , respectively. This is reasonable agreement

(2) Elkind, J. L.; Sunderlin, L. S.; Armentrout, P. B. *J. Phys. Chem.* **1989**, *93*, 3151–3158.

(3) Tolbert, M. A.; Beauchamp, J. L. *J. Am. Chem. Soc.* **1984**, *106*, 8117–8122.

(4) Sunderlin, L. S.; Armentrout, P. B. *J. Am. Chem. Soc.* **1989**, *111*, 3845–3855.

(5) Sunderlin, L.; Aristov, N.; Armentrout, P. B. *J. Am. Chem. Soc.* **1987**, *109*, 78–89.

(6) Lech, L. M.; Freiser, B. S. *Organometallics* **1988**, *7*, 1948–1957.

(7) Sunderlin, L. S.; Armentrout, P. B. *Int. J. Mass Spectrom. Ion Processes* **1989**, *94*, 149–177.

(8) Ervin, K. M.; Armentrout, P. B. *J. Chem. Phys.* **1985**, *83*, 166–189.

(9) Sunderlin, L. S.; Armentrout, P. B. *J. Phys. Chem.* **1988**, *92*, 1209–1219.

(10) Energy levels from: Sugar, J.; Corliss, C. *J. Phys. Chem. Ref. Data* **1985**, *14*, Suppl. 2.

(11) Chantry, P. J. *J. Chem. Phys.* **1971**, *55*, 2746–2759.

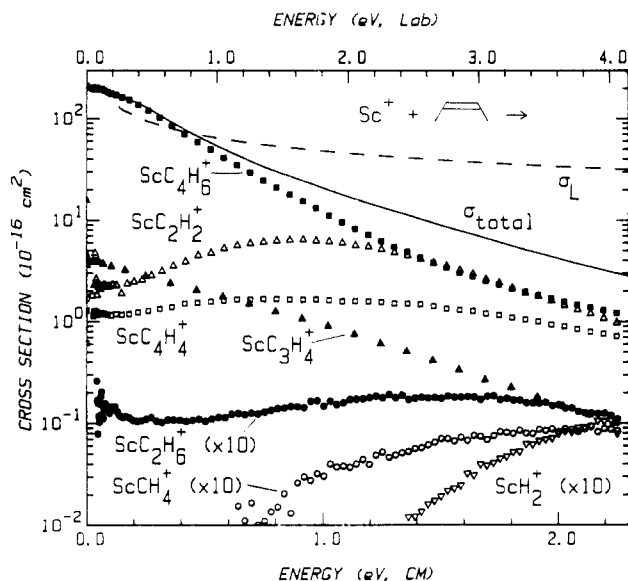
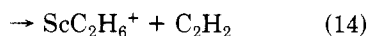
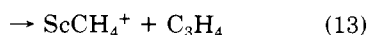
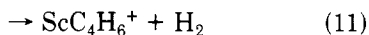
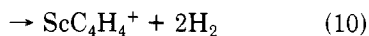
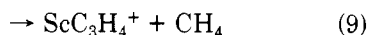
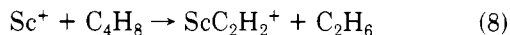


Figure 2. Variations of product cross sections with translational energy in the laboratory frame (upper axis) and center-of-mass frame (lower axis) for the reaction of Sc^+ with *cis*-2-butene.

with the TB data, although our total cross section at this energy is 3.7 \AA^2 . Similar differences in total cross sections and energy scale were found for studies of the reaction of Ti^+ with ethane and propane.⁷ Our measurements are probably more reliable due to the use of an octopole beam guide.

The reaction of Sc^+ with propane-2,2-*d*₂ was also studied. Our results for the exothermic reactions 4–7 are consistent with the previous results of Tolbert and Beauchamp.³ For reaction 1, both ScH^+ and ScD^+ are observed in a 2:1 ratio at 4 eV (largely reflecting the different numbers of protons and deuterons). For reaction 2, exclusive formation of ScHD^+ was seen in the threshold region. For reaction 3, only formation of ScCH_3^+ is observed.

***cis*- and *trans*-2-Butene.** Many products are formed in the reaction of Sc^+ with *cis*-2-butene and *trans*-2-butene. Product distributions for the two butenes are nearly identical. The major products at low kinetic energies (<3 eV) are formed in reactions 8–11. Three other products



of interest in this study are formed by reactions 12–14. Cross sections for these seven products for the interaction of Sc^+ with *cis*-2-butene are shown in Figure 2. Other products seen are ScCH_2^+ , ScCH_3^+ , ScC_2H_4^+ , ScC_3H_2^+ , and ScC_3H_5^+ . These reactions have cross sections of $\leq 0.2 \text{ \AA}^2$ between 0 and 4 eV. ScH^+ was not monitored because of mass overlap with the intense neighboring Sc^+ peak.

Reaction in this system is clearly more efficient than in the propane system. A comparison of the total cross section with σ_{L} indicates that reaction is $\approx 100\%$ efficient at low energy.¹² The major products are single and double

Table I. Literature Thermochemistry (298 K)^a

species	$\Delta_f H$, kcal/mol	species	$\Delta_f H$, kcal/mol
H	52.1 (0.0) ^b	C_3H_4 (propyne)	44.2 (0.2)
CH_2	92.3 (1.0) ^b	C_3H_8	-25.0 (0.1)
CH_3	34.8 (0.2) ^b	<i>cis</i> - C_4H_8	-1.7 (0.2)
CH_4	-17.8 (0.1)	<i>trans</i> - C_4H_8	-2.7 (0.2)
C_2H_2	54.5 (0.2)	<i>iso</i> - C_4H_{10}	-32.1 (0.2)
C_2H_4	12.5 (0.1)	<i>n</i> - C_4H_{10}	-30.0 (0.2)
C_2H_6	-20.0 (0.1)	Sc^+	243.1 (1.9) ^c

^a Unless noted values from: Pedley, J. M.; Naylor, R. D.; Kirby, S. P. *Thermochemical Data of Organic Compounds*; Chapman and Hall: London, 1986. ^b Chase, M. W., Jr.; Davies, C. W.; Downey, J. R., Jr.; Frurip, D. J.; McDonald, R. A.; Syverud, A. N. *J. Phys. Chem. Ref. Data* 1985, 14, Suppl. 1 (JANAF Tables). ^c Wagman, D. D.; et al. *J. Phys. Chem. Ref. Data* 1982, 11, Suppl. 2.

dehydrogenation and loss of methane and ethane, in direct parallel to the results for propane.

Lech and Freiser⁶ have previously studied this system at thermal energies using Fourier transform ion cyclotron resonance mass spectrometry and observed reactions 10 and 11 with a branching ratio of 7:93 (for both butenes). Other low-energy products were not reported. By comparison, we measure a branching ratio for reactions 8, 9, 10, and 11 of 1.1:2.2:0.6:96 at 0.1 eV, the lowest energy at which we can reliably derive branching ratios. In the experiments of Lech and Freiser, Sc^+ was generated by laser ablation, a process that tends to create more excited state ions than the SI source used here.¹³ It is likely that more highly excited ions have a greater probability of causing a second dehydrogenation of butene because of their higher energy content. This may explain the differences in the branching ratios from the two experiments.

Discussion

Thermochemistry. Theory and experiment indicate that cross sections can be parameterized in the threshold region by function 15.¹⁴ Here, E_0 is the threshold for

$$\sigma(E) = \sum_i g_i \sigma_0 (E - E_0 + E_i)^n / E \quad (15)$$

reaction of the lowest state of Sc^+ , E is the relative translational energy of the reactants, E_i is the electronic excitation of each specific electronic state, n is an adjustable parameter, g_i is the population of each state, and σ_0 is a scaling factor. The parameters σ_0 , n , and E_0 are optimized by using a nonlinear least-squares analysis to give the best fit to the data. Error limits for E_0 are calculated from the range in these threshold values for different data sets and the error in the absolute energy scale.

The threshold energies for endothermic reactions are converted to thermochemical values of interest by assuming that E_0 represents the enthalpy difference between reactants and products. This assumes that there are no activation barriers in excess of the endothermicity. This is generally true for ion-molecule reactions and has been explicitly tested a number of times.¹⁵ The derived en-

(12) Below about 0.4 eV, the measured total cross sections for *cis*-2-butene and *trans*-2-butene are somewhat higher than σ_{L} (by up to 40 and 20%, respectively, at 0.2 eV). The small dipole moment of *cis*-2-butene may explain why its cross section is larger than that for *trans*-2-butene. (Indeed, a locked dipole model predicts a cross section for the *cis* isomer that is 17% larger at 0.2 eV than that for the *trans* isomer.) Some of the discrepancy ($\approx 10\%$) with σ_{L} can be accounted for by correctly including the effects of the ion energy distribution. Any remaining discrepancies are within the 20% error limits for absolute cross sections.

(13) Kang, H.; Beauchamp, J. L. *J. Phys. Chem.* 1985, 89, 3364–3367. Loh, S. K.; Fisher, E. R.; Lian, L.; Schultz, R. H.; Armentrout, P. B. *J. Phys. Chem.* 1989, 93, 3159–3167.

(14) See discussion in ref 4.

Table II. Fitting Parameters for Eq 14

reaction	σ_0	n	E_0
$\text{Sc}^+ + \text{C}_3\text{H}_8 \rightarrow$ $\text{ScCH}_4^+ + \text{C}_2\text{H}_6$	0.21 (0.01)	0.52 (0.37)	0.20 (0.12)
$\text{Sc}^+ + \text{cis-C}_4\text{H}_8 \rightarrow$ $\text{ScCH}_4^+ + \text{C}_3\text{H}_4$	0.0095 (0.0001)	1.75 (0.09)	0.50 (0.06)
$\text{Sc}^+ + \text{trans-C}_4\text{H}_8 \rightarrow$ $\text{ScC}_2\text{H}_6^+ + \text{C}_2\text{H}_2$	0.019 (0.001)	1.34 (0.06)	0.40 (0.05)
$\text{Sc}^+ + \text{trans-C}_4\text{H}_8 \rightarrow$ $\text{ScCH}_4^+ + \text{C}_3\text{H}_4$	0.016	1.92	0.66 (0.06)
$\text{Sc}^+ + \text{trans-C}_4\text{H}_8 \rightarrow$ $\text{ScC}_2\text{H}_6^+ + \text{C}_2\text{H}_2$	0.072 (0.007)	1.36 (0.50)	0.48 (0.11)

thalpies of formation of products can be used to derive bond energies where the structure of the product can be determined. We assume that the neutral reactants and the products formed at the threshold of an endothermic reaction are characterized by a temperature of 298 K in all degrees of freedom. Thus, we make no correction for the energy available in internal modes of the neutral reactant. Hydrocarbon thermochemistry needed below is given in Table I, and the fitting parameters for eq 15 are given in Table II.

1. ScCH_4^+ . The threshold for formation of ScCH_4^+ in the reaction with propane, process 4, is 0.20 ± 0.12 eV. This is consistent with the reported threshold for this reaction of 0.5 ± 0.5 eV reported by TB.³ Our threshold leads to $\Delta_f H(\text{ScCH}_4^+) = 210 \pm 4$ kcal/mol. The thresholds for reaction 13 of 0.50 ± 0.06 and 0.66 ± 0.06 eV with *cis*- and *trans*-2-butene, respectively, give $\Delta_f H(\text{ScCH}_4^+) = 209 \pm 3$ and 211 ± 3 kcal/mol. Combining all data gives an average value of $\Delta_f H(\text{ScCH}_4^+) = 210 \pm 3$ kcal/mol.

2. ScC_2H_6^+ . The reaction of Sc^+ with isobutane to form ScC_2H_6^+ is exothermic,^{3,16} indicating that $\Delta_f H(\text{ScC}_2\text{H}_6^+) \leq 199 \pm 2$ kcal/mol. The cross section at 0.1 eV is 6% of the Langevin cross section.¹⁶ This is sufficiently large to suggest (although not unambiguously) that the ground state of Sc^+ does react exothermically. A similar exothermic cross section that is 20% of σ_L (and thus must be due, at least in part, to the ground state) is seen for formation of ScC_2H_6^+ from *n*-butane.¹⁶ This means $\Delta_f H(\text{ScC}_2\text{H}_6^+) \leq 201 \pm 2$ kcal/mol. Cross sections for formation of ScC_2H_6^+ in reactions with *cis*- and *trans*-2-butene include small exothermic features and endothermic features starting at low energy. The exothermic features can be attributed to electronically excited Sc^+ ions. Modeling of the cross section therefore includes both exothermic and endothermic contributions. The exothermic features for both butenes can be modeled by a function of the form $(0.008 \pm 0.003)E^{-0.47 \pm 0.15}$, a form similar in shape to σ_L . The endothermic features are modeled by using eq 15 and the parameters given in Table II. Note that the thresholds derived (0.40 and 0.48 eV) mean that $\text{Sc}^+(\text{1D})$ excited state at 0.315 eV reacts endothermically, but the $\text{Sc}^+(\text{3F})$ at 0.61 eV can react exothermically. Other assumptions about which states react exothermically are incompatible with the thresholds derived. The threshold analyses for *cis*- and *trans*-2-butene give 196 ± 2 and 197 ± 4 kcal/mol for $\Delta_f H(\text{ScC}_2\text{H}_6^+)$, respectively. These results are consistent with the limit derived from the butane data.

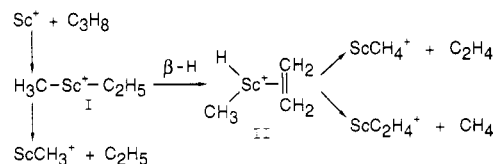
3. **Other Thermochemistry.** Thermochemical data for many of the other products seen in these studies have been measured previously (Table III) and therefore will

Table III. Sc^+ -Ligand Bond Energies

bond(s)	D°_{298} , kcal/mol	bond(s)	D°_{298} , kcal/mol
Sc^+-H	57.2 ± 2.1^a	Sc^+-CH_3	116.9 ± 1.6^d
Sc^+-CH_2	98.5 ± 5.3^b	$\text{H}_3\text{CSc}^+-\text{CH}_3$	
Sc^+-CH_3	59.0 ± 3.0^c	$\text{Sc}^+-\text{C}_2\text{H}_2$	77.9 ± 2.3^c
$\text{Sc}^+-\text{H} + \text{HSc}^+-\text{H}$	115.5 ± 3.0^c	$\text{Sc}^+-\text{C}_2\text{H}_4$	$\geq 35.0 \pm 1.2^c$
$\text{Sc}^+-\text{H} + \text{HSc}^+-\text{CH}_3$	120.3 ± 2.1^d	$\text{Sc}^+-\text{C}_4\text{H}_6$	$\geq 29^d$

^a Reference 2. ^b Reference 4. ^c Reference 5. ^d This work. ^e Reference 6.

Scheme I



not be discussed in detail here. Analyses of reactions 2 and 3 have been reported previously as part of the thermochemical characterization of ScH_2^+ and ScCH_3^+ .⁵ Thermochemistry for ScC_3H_4^+ , ScC_3H_6^+ , and ScC_4H_4^+ has not been previously obtained and is discussed here. Since structures of these species are ambiguous, with metallocycle and metal-alkene/alkyne structures both feasible, only heats of formation can be derived from our data.

Given the thermochemistry in Table I, the exothermicity of reaction 7 provides an upper limit of $\Delta_f H(\text{ScC}_3\text{H}_6^+) \leq 218 \pm 2$ kcal/mol. The exothermicity of reaction 9 gives an upper limit of $\Delta_f H(\text{ScC}_3\text{H}_4^+) \leq 258 \pm 2$ kcal/mol. Reaction 6 is apparently endothermic with a very low threshold. Good fits to the data cannot be found for thresholds higher than 0.2 eV. We conservatively hold that the threshold is 0.10 ± 0.20 eV because strong competition with the other exothermic products may greatly affect the cross-section shape. This indicates $\Delta_f H(\text{ScC}_3\text{H}_4^+) = 220 \pm 5$ kcal/mol. If the structure of this product is Sc^+ -propyne,¹⁷ then $D^\circ(\text{Sc}^+-\text{C}_3\text{H}_4) = 67 \pm 5$ kcal/mol, somewhat lower than $D^\circ(\text{Sc}^+-\text{ethyne}) = 78 \pm 2$ kcal/mol.⁵

The thresholds for reaction 10 of 0.13 ± 0.06 eV for both butenes suggest $\Delta_f H(\text{ScC}_4\text{H}_4^+) = 244 \pm 2$ kcal/mol.¹⁸ $\Delta_f H(\text{ScC}_2\text{H}_2^+ + \text{C}_2\text{H}_2)$ is 274 ± 3 kcal/mol, only 31 ± 3 kcal/mol above $\Delta_f H(\text{ScC}_4\text{H}_4^+)$. Since $D^\circ(\text{Sc}^+-\text{C}_2\text{H}_2) = 78 \pm 2$ kcal/mol, it is unlikely that $D^\circ(\text{C}_2\text{H}_2\text{Sc}^+-\text{C}_2\text{H}_2)$ is only 31 kcal/mol. Thus, the ScC_4H_4^+ species seen in this experiment is most likely another structural isomer (such as a metallocyclopentadiene¹⁹) or involves a barrier to forming the bisethyne.

Reaction Mechanisms and Efficiencies. The mechanisms for the reactions discussed here are similar to those discussed previously for the reactions of Sc^+ with other hydrocarbons^{3,5} and for the reaction of Ti^+ with *trans*-2-butene.⁷ All major products seen in the systems studied here can be explained by using the elementary reaction steps of oxidative addition of C-H or C-C bonds to the metal, followed by β -hydrogen, γ -hydrogen, or β -methyl migration, and then reductive elimination or direct bond cleavage.⁵ Scheme I shows such a mechanism for the C-C bond cleavage products in the propane system (analogous

(17) If Sc^+ -allene were the product, then $D^\circ(\text{Sc}^+-\text{C}_3\text{H}_4) = 69 \pm 5$ kcal/mol. Since this value is probably quite a bit higher than $D^\circ(\text{Sc}^+-\text{C}_2\text{H}_4)$ (Table III), the propyne complex seems the more likely structure.

(18) Evidence for two stable isomers of ScC_4H_4^+ is reported in ref. 6.

(19) Studies of isotopically labeled butane⁹ suggest that double dehydrogenation of butane leads to a metal-butadiene complex. Dehydrogenation of this species (which can be formed from butene as well) could easily lead to a cyclic product. See also ref. 6.

(15) Boo, B. H.; Armentrout, P. B. *J. Am. Chem. Soc.* **1987**, *109*, 3549-3559. Ervin, K. M.; Armentrout, P. B. *J. Chem. Phys.* **1987**, *86*, 2659-2673. Elkind, J. L.; Armentrout, P. B. *J. Phys. Chem.* **1984**, *88*, 5454-5456. Armentrout, P. B. In *Structure/Reactivity and Thermochemistry of Ions*; Ausloos, P., Lias, S. G., Eds.; D. Reidel: Dordrecht, 1987; pp 97-164.

(16) Sunderlin, L. S.; Armentrout, P. B., unpublished results.

mechanisms have been proposed for reaction of Sc^+ with ethane and butane).^{3,5} Note that reversible insertion into an allylic C–H bond can readily lead to interconversion of *cis*- and *trans*-2-butene,⁷ in accordance with the equivalence of the experimental results for these isomers.

One consequence of this mechanism concerns whether there are any barriers in excess of the endothermicity for the reactions analyzed. Since formation of ScC_2H_4^+ is exothermic (Figure 1), there can be no barriers to formation of intermediates I and II in Scheme I. Since elimination of C_2H_4 from II is a simple metal–ligand bond cleavage, there should be no barrier to that step either. Thus, there can be no barrier higher than the endothermicity at any point in the reaction pathway for reaction 4. Similar arguments indicate that the thresholds for reactions 13 and 14 also are the true thermodynamic thresholds.

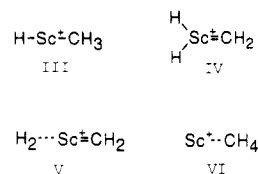
Another consequence of this mechanism is the implied competition between the various products, for example, ScCH_4^+ and ScC_2H_4^+ (Scheme I). Indeed, we find that the sum of the cross sections for these products yields a smooth curve, consistent with such a competition. Similar results are obtained for other such pairs of products.

One of the interesting observations made by TB was that Sc^+ induces both 1,2- and 1,3-hydrogen elimination from propane.³ Our results for deuterium-labeled propane are completely consistent with this, indicating that 60% 1,2- and 40% 1,3-dehydrogenation occur. Thus, the ScC_3H_6^+ product of reaction 7 is apparently a mixture of Sc^+ -propene after 1,2-elimination of hydrogen and a metallocyclobutane after 1,3-elimination of hydrogen. Exothermic production of both of these species is thermodynamically reasonable. In our work, we also find that reaction 2 with 2,2-deuterated propane results in exclusive formation of ScHD^+ , indicating that the neutral product is propene and not cyclopropane. This is verified by the thermochemistry. On the basis of bond energies for the ScH_2^+ product that are derived from reaction with ethane, cyclopentane, and cyclohexane,⁵ and threshold for reaction 2 corresponds with propene loss rather than cyclopropane loss, 8 kcal/mol higher in energy. This also makes sense mechanistically. While elimination of propane is a simple fission of a dative bond, elimination of cyclopropane requires formation of a C–C bond (via a tight transition state). Thus, propene elimination can compete effectively with reductive elimination of H_2 while loss of cyclopropane is both kinetically and thermodynamically less favorable.

Finally, we need to explain the difference in reaction efficiency for the propane and butene systems. We have previously postulated that the reaction of Sc^+ and ethane is inefficient (1.7%) because of the need to change spin during the oxidative addition step of the reaction.⁵ A similar change in spin is required in the propane and butene systems. The efficiency of this process is strongly influenced by the strength of the initial ion–molecule interaction, since a deeper well leads to less competition from dissociation back to reactants. In the case of ethane and propane, this is determined by the ion–induced dipole attraction, which scales with the polarizability of the alkane. Since propane is more polarizable than ethane, the reaction efficiency is enhanced. For butene, the polarizability is still larger and there is a significant interaction between the ion and the π bond, about $D^\circ(\text{Sc}^+-\text{C}_2\text{H}_4) \geq 35 \pm 1$ kcal/mol.⁵ Thus, the butene reaction nears 100% efficiency.

Structures. 1. ScCH_4^+ . To obtain bond energies from the heats of formation derived above, the structures of the ions formed must be determined. For ScCH_4^+ , there are

four possible structures, III–VI. Structure III is the most



obvious since it is implied by the mechanism of Scheme I and therefore is kinetically reasonable. III is also thermodynamically reasonable since this structure implies that $D^\circ(\text{Sc}^+-\text{H}) + D^\circ(\text{HSc}^+-\text{CH}_3) = 120 \pm 2$ kcal/mol, a value that is similar to our previously reported value of $D^\circ(\text{Sc}^+-\text{H}) + D^\circ(\text{HSc}^+-\text{H}) = 116 \pm 3$ kcal/mol. Since $D^\circ(\text{Sc}^+-\text{H}) \approx D^\circ(\text{Sc}^+-\text{CH}_3)$ (Table III), this agreement indicates that structure III is consistent with the thermochemistry.

Structure IV can be ruled out on thermodynamic grounds, since the measured heat of formation combined with known thermochemical data would indicate $D^\circ(\text{H}_2\text{Sc}^+-\text{CH}_2) = 114 \pm 4$ kcal/mol. This is significantly larger than $D^\circ(\text{Sc}^+-\text{CH}_2) = 98 \pm 5$ kcal/mol. Since Sc^+ has only two valence electrons, covalently bound ScH_2^+ has no unpaired electrons remaining to bond to CH_2 . It therefore seems unreasonable that $D^\circ(\text{H}_2\text{Sc}^+-\text{CH}_2)$ should be greater than $D^\circ(\text{Sc}^+-\text{CH}_2)$, since the latter species has a covalent double bond.^{1,4}

Structure V avoids the problem of having too few valence electrons on Sc^+ . If this is the species formed in reactions 4 and 13, then $D^\circ(\text{H}_2\text{CSc}^+-\text{H}_2) = 27 \pm 6$ kcal/mol. This number is high for an ion–induced dipole bond between two closed-shell species since the polarizability of H_2 is very small. This is illustrated by the calculations of Rappé and Upton²⁰ on the SeH_2^+ potential energy surface, which shows no significant Sc^+-H_2 well.

If structure VI is the product formed in reaction 4, then the thermochemical implication is $D^\circ(\text{Sc}^+-\text{CH}_4) = 17 \pm 2$ kcal/mol. While this is a more reasonable ion–induced dipole bond strength, it cannot easily explain the observed competition between reactions 4 and 5, since the immediate precursor to VI must be $\text{CH}_4-\text{Sc}^+-\text{C}_2\text{H}_4$ (an isomer of II). Since $D^\circ(\text{Sc}^+-\text{C}_2\text{H}_4) > 35 \pm 1$ kcal/mol $> D^\circ(\text{Sc}^+-\text{CH}_4)$, we expect formation of ScC_2H_4^+ to dominate. While this is true at lower energies, above 1 eV (Figure 1), the cross section for ScCH_4^+ is significantly larger than the cross section for ScC_2H_4^+ . This means that the former process is kinetically favored, a result that is inconsistent with the $\text{CH}_4-\text{Sc}^+-\text{C}_2\text{H}_4$ intermediate since both reactions occur via direct bond cleavage processes. (This scenario contrasts with that shown in Scheme I. Here, formation of III from II is kinetically favored since it occurs via reductive elimination of CH_4 , a process that requires a tight transition state.) Hence, structure VI can also be discounted, leaving III as the most reasonable structure.

2. ScC_2H_6^+ . The possible isomers for ScC_2H_6^+ have been previously discussed by TB,³ who on thermodynamic grounds concluded that the dimethyl species is the most reasonable product. Reaction with butane-1,1,1,4,4,4-*d*₆ showed formation of ScC_2D_6^+ dominating formation of other isotopomers.³ This is a strong indication that the dimethyl species is a product of the reaction with butane. The same thermochemical arguments hold for reaction 14. The dynamics of formation of ScC_2H_6^+ with butane and butene should also be reasonably similar, such that we presume that the ScC_2H_6^+ formed in reaction 14 is indeed the dimethyl species. Note that reactions 12, 13, and 14

can then be explained by essentially identical mechanisms, with the only difference being whether hydride or methyl ligands are taken by the metal. This mechanism is analogous to that shown in Scheme I. The thermochemical implication of this structure and our heat of formation data is $D^\circ(\text{Sc}^+-\text{CH}_3) + D^\circ(\text{CH}_3\text{Sc}^+-\text{CH}_3) = 117 \pm 2$ kcal/mol. Again the similarity of this bond energy sum to those for ScH_2^+ and ScCH_4^+ is consistent with the assigned structures. Theoretical calculations give $D^\circ(\text{Sc}^+-\text{CH}_3) + D^\circ(\text{CH}_3\text{Sc}^+-\text{CH}_3) = 108$ kcal/mol, in reasonable agreement with the experimental value.²¹

"Intrinsic" First and Second Metal-Ligand Bond Energies. Recent models of metal-ligand bond strengths show that periodic trends in metal-hydrogen and metal-methyl bond strengths can be quantitatively correlated with the promotion energy, the energy necessary to promote the atomic ion into a state suitable for bonding.^{1,22} The most useful correlations find that this bonding state has an sd^{n-1} orbital occupancy with the bonding electron of the metal (largely an s electron for the first bond and a d electron for subsequent bonds) spin-decoupled from the other electrons on the metal. Recent calculations of promotion energies indicate that in the case of Sc^+ , the first bond promotion energy is 4 kcal/mol.²² No further promotion is necessary to make a second bond. Thus, the second metal-ligand bond energy for Sc^+ , $D^\circ(\text{RSc}^+-\text{R})$, is anticipated to equal the "intrinsic" metal-ligand bond energy (the highest value expected in the absence of electronic and steric effects), ≈ 58 kcal/mol.¹ Indeed, the data in Table III can be used to calculate the four second-ligand bond strengths, $D^\circ(\text{HSc}^+-\text{H}) = 58$ kcal/mol, $D^\circ(\text{H}_3\text{CSc}^+-\text{H}) = 61$ kcal/mol, $D^\circ(\text{HSc}^+-\text{CH}_3) = 63$ kcal/mol, and $D^\circ(\text{H}_3\text{CSc}^+-\text{CH}_3) = 58$ kcal/mol, all in agreement with the promotion energy model. For comparison, the sums of the two bond energies for $\text{Ti}(\text{CH}_3)_2^+$ and $\text{V}(\text{CH}_3)_2^+$ have been found to be 118 ± 6^7 and $98 \pm$

5 kcal/mol,²³ respectively. These values also fit the promotion energy model reasonably well, as has been discussed recently.^{1,23}

Implications for Insertion Reactions. The two-ligand bond strength sums given in Table III indicate that insertion of Sc^+ into an H-H bond, a C-H bond of methane, and a C-C bond of ethane are exothermic by 11 ± 3 , 16 ± 2 , and 27 ± 2 kcal/mol, respectively. Given the relatively small range in H-C and C-C bond strengths of saturated hydrocarbons, this indicates that oxidative addition of C-H and C-C bonds to Sc^+ should be exothermic for all alkanes.

This conclusion for Sc^+ can be extended to other species by noting that the Sc^+-R and RSc^+-R bond strengths ($\text{R} = \text{H}$ or CH_3) are close to the "intrinsic" bond strengths, since the first and second promotion energies of Sc^+ are small. We have argued previously¹ that such intrinsic bond energies are useful as starting points to estimate the bond energies in condensed-phase organometallic complexes. Steric and electronic effects must then also be estimated. Carter and Goddard have provided a quantitative approach to estimating such electronic effects.²² Overall, we expect that it is thermodynamically favorable to oxidatively add hydrocarbon bonds to metal centers with two unpaired electrons in orbitals suitable for bonding and with little or no steric hindrance.

Acknowledgment. This research is funded by the National Science Foundation, Grant CHE-8796289 and CHE-8917980. L.S.S. thanks the NSF for a Predoctoral Fellowship, 1985-1988.

Registry No. Sc, 22537-29-7; C_3H_8 , 74-98-6; *cis*- C_4H_8 , 590-18-1; *trans*- C_4H_8 , 624-64-6.

Supplementary Material Available: Cross section plots for minor products with propane and *cis*-2-butene and all products for *trans*-2-butene (5 pages). Ordering information is given on any current masthead page.

(21) Bauschlicher, C. W., personal communication.

(22) Carter, E. A.; Goddard, W. A. *J. Phys. Chem.* **1988**, *92*, 5679-5683.

(23) Armentrout, P. B. In *ACS Symp. Ser.*, Marks, T. J., Ed., in press.